




The canonical RdDM pathway mediates the control of seed germination timing under salinity

Víctor Miguel Palomar^{1,†} , Alejandro Garcarrubio², Adriana Garay-Arroyo³, Coral Martínez-Martínez¹, Omar Rosas-Bringas¹, José L. Reyes¹  and Alejandra A. Covarrubias^{1,*} 

¹Departamento de Biología Molecular de Plantas, Instituto de Biotecnología, Universidad Nacional Autónoma de México, Apdo. Postal 510-3, Cuernavaca, Mor. C.P 62250, Mexico,

²Departamento de Ingeniería Celular y Biotecnología, Instituto de Biotecnología, Universidad Nacional Autónoma de México, Apdo. Postal 510-3, Cuernavaca, Mor. C.P 62250, Mexico, and

³Laboratorio de Genética Molecular, Desarrollo y Evolución de Plantas, Instituto de Ecología, Universidad Nacional Autónoma de México, Circuito Exterior S/N anexo Jardín Botánico Exterior, Ciudad Universitaria, Ciudad de México C.P. 04500, México

Received 8 February 2018; revised 11 September 2020; accepted 26 October 2020; published online 1 November 2020.

*For correspondence (e-mail crobles@ibt.unam.mx).

†Present address: Department of Molecular, Cellular and Developmental Biology, University of Michigan, Ann Arbor, Michigan, USA

SUMMARY

Plants respond to adverse environmental cues by adjusting a wide variety of processes through highly regulated mechanisms to maintain plant homeostasis for survival. As a result of the sessile nature of plants, their response, adjustment and adaptation to the changing environment is intimately coordinated with their developmental programs through the crosstalk of regulatory networks. Germination is a critical process in the plant life cycle, and thus plants have evolved various strategies to control the timing of germination according to their local environment. The mechanisms involved in these adjustment responses are largely unknown, however. Here, we report that mutations in core elements of canonical RNA-directed DNA methylation (RdDM) affect the germination and post-germination growth of Arabidopsis seeds grown under salinity stress. Transcriptomic and whole-genome bisulfite sequencing (WGBS) analyses support the involvement of this pathway in the control of germination timing and post-germination growth under salinity stress by preventing the transcriptional activation of genes implicated in these processes. Subsequent transcriptional effects on genes that function in relation to these developmental events support this conclusion.

Keywords: RdDM pathway, AGO4 protein, germination, Arabidopsis, RNA-directed DNA methylation, salinity.

INTRODUCTION

Different mechanisms are involved in the tuning of an efficient and appropriate gene expression program under stressful conditions. Among the best-characterized control mechanisms are those modulating transcription patterns that involve pathways controlling the number and/or activity of different transcription factors (Zhu, 2002; Yamaguchi-Shinozaki and Shinozaki, 2006; Nakashima *et al.*, 2009). More recently, additional mechanisms involving chromatin modifications, some of them persistent and/or heritable, have been implicated in the modulation of transcriptional activity denoting epigenetic regulation (Cubas *et al.*, 1999; Soppe *et al.*, 2000; Manning *et al.*, 2006; Pecinka and Mittelsten Scheid, 2012). Transcriptional control of gene

expression is also exerted through the recruitment of histone variants to different genome regions, histone post-translational modifications and DNA methylation, which leads to the conformation of a wide variety of 'epigenomes' depending on developmental or environmental signals, or those derived from their crosstalk.

Plants have evolved under frequent and/or sudden environmental changes; hence, the control of their developmental programs has co-evolved with their stress responses to be able to develop, grow and reproduce under adverse conditions (Skirycz and Inze, 2010). The ability to acclimate upon repeated exposure to a particular stress is frequently observed in plants, with such a response representing a form of short-term stress memory (Chinnusamy and Zhu, 2009; Secco *et al.*, 2015). This

capacity to retain a stress memory also occurs for longer periods (Molinier *et al.*, 2006; Chinnusamy and Zhu, 2009; Han and Wagner, 2014). Diverse processes that lead to stable DNA methylation and histone modifications have been identified in this behavior, allowing growth adjustment and reprogramming of developmental decisions (Chinnusamy and Zhu, 2009; Han and Wagner, 2014; Kinoshita and Seki, 2014).

DNA methylation is considered an essential plant contention mechanism against transposable element activation, which may occur under hostile conditions such as high temperatures (Ito *et al.*, 2011; Matsunaga *et al.*, 2012). The extent of plant genome methylation is controlled by new/novel and maintenance DNA methylation, and by demethylation processes. DNA methylation may occur in symmetric (CG and CHG) and asymmetric (CHH) sequence contexts (H = C, A or T) (Law and Jacobsen, 2010). To date, four DNA methylation writers have been described in *Arabidopsis*: DNA METHYL TRANSFERASE 1 (MET1), responsible for maintaining CG methylation; CHROMOMETHYLASE 3 (CMT3), which retains methylation in CHG contexts; CMT2, which retains methylation in CHG and CHH sequences; and RNA-directed DNA methylation (RdDM), which mediates the initiation and maintenance of DNA methylation, mostly at CHH sites and to a lesser extent at CG and CHG sequences, with the participation of DOMAINS REARRANGED METHYLTRANSFERASE 2 (DRM2) and other context-specific methyltransferases (Law and Jacobsen, 2010).

RNA-directed DNA methylation (RdDM) consists of complex pathways occurring through the participation of small interfering RNAs (siRNAs) and requires a specific transcriptional assembly. The best-characterized RdDM pathway, known as canonical RdDM, depends on two plant-specific RNA polymerases, Pol IV and Pol V, which play key roles (Mahfouz, 2010; Matzke *et al.*, 2015; Wang and Axtell, 2017), together with RNA-DEPENDENT RNA POLYMERASE 2 (RDR2), type-III ribonuclease DICER-LIKE 3 (DCL3) (Henderson *et al.*, 2006; Blevins *et al.*, 2015; Zhai *et al.*, 2015) and ARGONAUTE 4 (AGO4) (Zilberman *et al.*, 2003), among other factors. RdDM is not exclusively a nuclear process, as siRNAs produced in the nucleus are exported to the cytoplasm (Ye *et al.*, 2012), where they are bound by AGO4 to then return to the nucleus to form a silencing complex by pairing with a scaffold long non-coding RNA produced by Pol V (Wierzbicki *et al.*, 2009; reviewed extensively by Matzke and Mosher, 2014; Matzke *et al.*, 2015). For the canonical RdDM pathway, there is evidence indicating that the formation of mature AGO4/siRNA complexes requires AGO4 endonucleolytic activity, which triggers the removal of the passenger strand, allowing entry of the mature AGO4/siRNA complex to the nucleus (Ye *et al.*, 2012). AGO4 is closely related to AGO6 and AGO9, proteins belonging to the same AGO family,

and has been shown to control DNA methylation through canonical and non-canonical RdDM pathways. AGO9 has a specific function by silencing transposable elements in the female gametophyte by a non-cell autonomous mechanism (Olmedo-Monfil *et al.*, 2010). Although AGO6 also participates in controlling DNA methylation via AGO6/RdDM and non-canonical AGO6/RDR6 RdDM pathways, AGO4 and AGO6 have different preferences for siRNAs (Havecker *et al.*, 2010; McCue *et al.*, 2015). Genome-wide methylation analyses of *ago4*, *ago6* or *ago4 ago6* mutants showed that there is very low redundancy between these proteins, indicating that they do not have exactly the same function, although they show some common targets (Havecker *et al.*, 2010; Eun *et al.*, 2011; Duan *et al.*, 2015; McCue *et al.*, 2015).

The participation of the RdDM pathway in different plant processes is exposed by phenotypes found in various plant species, including *Zea mays* (maize; Hollick, 2010), *Oryza sativa* (rice; Wu *et al.*, 2010; Wei *et al.*, 2014), *Solanum lycopersicum* (tomato; Gouil and Baulcombe, 2016; Corem *et al.*, 2018), and two Brassicaceae species, *Brassica rapa* (Grover *et al.*, 2018) and *Capsella rubella* (Wang *et al.*, 2020). However, although dynamic DNA methylation occurs during different developmental stages, in the absence of RdDM core proteins few phenotypes have been detected in *Arabidopsis thaliana* plants growing under optimal conditions (Matzke *et al.*, 2015). Among these are a delay in flowering time (Pontier *et al.*, 2005; Haag and Pikaard, 2011), the anomalous expression of imprinted genes leading to seed arrest (triploid block; Kradolfer *et al.*, 2013; Borges *et al.*, 2018; Martinez *et al.*, 2018) and defects in endosperm development (Köhler and Lafon-Placette, 2015; Chow *et al.*, 2020). In addition, a role for RdDM during pathogen infection has been evidenced by the phenotypes of RdDM-associated protein mutants during infection by viruses (Hamera *et al.*, 2012; Yang *et al.*, 2013; Brosseau *et al.*, 2016), bacteria (Agorio and Vera, 2007; Downen *et al.*, 2012; Gohlke *et al.*, 2013) or fungi (Lopez *et al.*, 2011; Le *et al.*, 2014). The RdDM pathway is also involved in the plant response to abiotic stresses such as heat (Ito *et al.*, 2011; Popova *et al.*, 2013), low relative humidity (Tricker *et al.*, 2012) and low temperatures (Chan *et al.*, 2016).

Germination is a crucial developmental stage in the plant life cycle, when plant embryos confront severe environmental changes: in orthodox seeds, when embryos switch from dry to humid conditions, or during embryo revival in unfavorable environments. Recently it was reported that DNA methylation is dynamically modulated during seed development and germination in *A. thaliana* under optimal conditions, where major changes occur in the methylation of the CHH sequence context (Kawakatsu *et al.*, 2017). In this work, we address the question of whether the canonical RdDM pathway is required for the proper germination of *A. thaliana* under conditions of high

salinity, a common condition present in arid and semi-arid regions, in degraded croplands and in contaminated soils. We demonstrate that the RdDM pathway plays a key role in the plant response to salinity during germination and early seedling growth. Accordingly, RNA-seq comparative analyses from wild-type plants and *AGO4* null and weak mutants, germinated in media with or without NaCl, show that in response to salinity RdDM is mostly involved in the control of embryo development and germination genes, and to a lesser degree in the regulation of genes implicated in stress tolerance. Whole-genome bisulfite sequencing (WGBS) analyses support the conclusion that this response is a consequence of the RdDM pathway modulating gene expression, mainly by controlling DNA methylation on its usual targets and preventing the activation of genes in response to salinity. These results agree with changes in the protein levels and localization of RdDM components during Arabidopsis germination and early seedling growth under this environmental adversity.

RESULTS

The canonical RdDM pathway is required for optimal germination under salinity stress

As there is evidence of a dynamic reprogramming of DNA methylation during seed development and germination and considering that germination is a critical process that repeatedly exposes the embryonic plant to extremes, we asked whether the RdDM pathway is involved in the plant response to salinity. To address this, we evaluated the germination rate of different mutant lines lacking the core proteins of the canonical RdDM pathway: DCL3, RDR2, and the largest subunits of Pol IV (NRPD1) and Pol V (NRPE1) (Matzke and Mosher, 2014). Under optimal conditions, all wild-type Arabidopsis (Col-0) and mutant lines germinated at similar rates, reaching 100% germination (Figure S1a). In contrast, when the seeds of these mutants were germinated under high salt concentration (250 mM NaCl), their germination rate significantly decreased ($P = 1e^{-4}$)

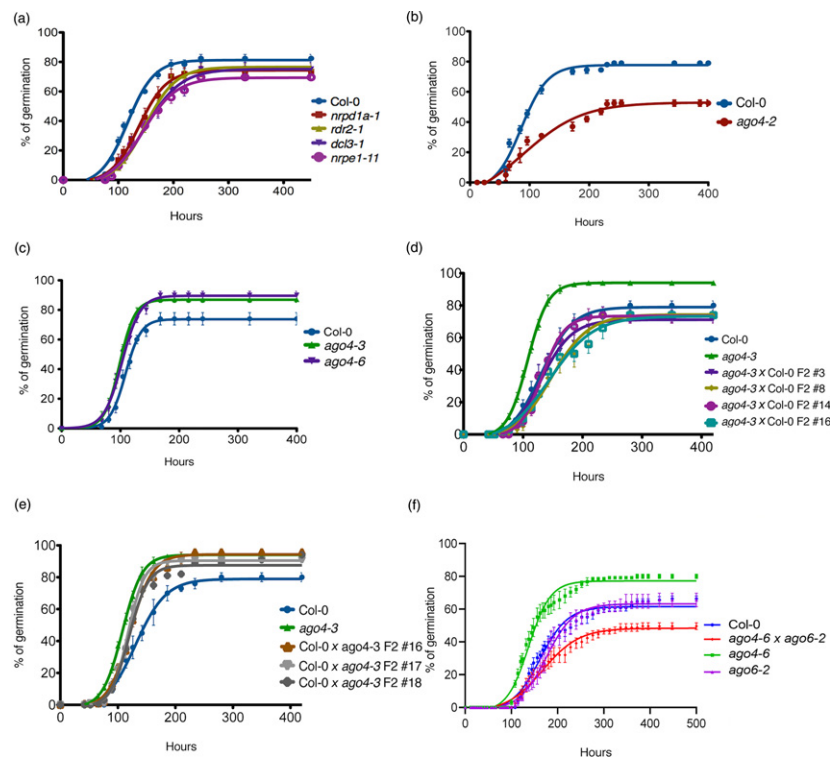


Figure 1. RNA-directed DNA methylation (RdDM) and ARGONAUTE 4 (AGO4) are required for the germination process under salt stress. (a–f) Arabidopsis seed germination curves in media containing 250 mM NaCl. (a) Comparison between RdDM core component mutant (*nrpd1a-1*, *rdr2-1*, *dcl3-1* and *nrpe1-11*) and wild-type (Col-0) lines ($P = 1e^{-4}$), under the Col-0 background. Differences between *nrpe1-11* and *nrpd1a-1*, and between *nrpe1-11* and *rdr2-1*, were also significant ($P = 1e^{-4}$ and $P = 3e^{-4}$, respectively). (b) Germination of *ago4-2* (point mutant allele) compared with the wild type (Col-0; $P = 1e^{-4}$). (c) Comparison between two *AGO4* null mutant alleles (*ago4-3* and *ago4-6*) and the wild type (Col-0; $P = 1e^{-4}$), under the Col-0 background. (d) Germination rate and capacity of *ago4-3* complementation lines compared with mutant and wild-type (Col-0) lines ($P = 1e^{-4}$). The wild-type allele was introduced by crossing into *ago4-3* homozygous plants and the resultant F₂ plants (homozygous for the wild-type allele) were used for the experiment. (e) Germination rate and capacity of *ago4-3* introgression lines compared with the *ago4-3* mutant and the wild type (Col-0; $P = 1e^{-4}$). The *ago4-3* mutant allele was introduced into wild-type plants by genetic crosses and the resultant F₂ plants (homozygous for the mutant allele *ago4-3*) were used for the experiment. (f) Comparison between wild type (Col-0), *ago4-6* and *ago6-2* single mutants, and *ago4-6 ago6-2* double mutant (homozygous for both mutant alleles; $P = 1e^{-4}$). The germination analyses under optimal conditions are shown in Figure S1.

compared with the wild type (Figure 1a), indicating that the canonical RdDM pathway is required for proper germination under conditions of high salinity.

Given this evidence, under the same conditions we analyzed seeds carrying an AGO4 point mutation allele (*ago4-2*; E641K within the PIWI domain, close to the residues required for AGO4 slicing activity), which behaves as a dominant-negative allele and causes defective DNA methylation by producing a less active protein, according to Agorio and Vera (2007). The results showed that *ago4-2* seeds present lower germination rates under salt stress, when compared with wild-type seeds (Figure 1b), consistent with the phenotype shown by the other RdDM-defective mutants (Figure 1a), although its germination profile under optimal conditions is only slightly changed (Figure S1b). This result confirms that the whole canonical RdDM is involved in germination under these environmental conditions.

As a phenotype similar to that of *ago4-2* would be expected for a mutant lacking AGO4 as part of the RdDM pathway, we analyzed the effect of the absence of AGO4 protein on germination efficiency under salt stress using a null AGO4 mutant (*ago4-3*). In sharp contrast to the negative effect on germination observed for the rest of the mutants (Figure 1a,b), under salt stress the lack of AGO4 protein led to a higher germination rate when compared with wild-type seeds (Col-0; Figure 1c). The same effect was detected for other AGO4 null mutant alleles (*ago4-6*; Figure 1c), some of them in different genetic backgrounds (*ago4-1*, *Ler* ecotype; *ago4-4*, *Ws* ecotype; Figure S2a,b, respectively). These AGO4 null alleles also reached similar germination efficiency compared with the wild type under optimal conditions (Figure S1c–e). The absence of the AGO4 protein in the different null mutants was confirmed by Western blot experiments (Figure S3). The salt concentration dependence of the germination phenotype in the absence of these RdDM components was also tested (germination under 150 and 200 mM NaCl), showing that the germination rate decreased in the null mutants of the RdDM pathway, as well as in the point mutant *ago4-2*; meanwhile, the germination of the three null *ago4* mutants increased compared with the wild type, as expected (Figure S4a–h), confirming that the observed phenotypes result from salt exposure.

To validate the contribution of AGO4 to the observed phenotypes, the wild-type gene was introduced into the *ago4-3* null mutant by genetic crosses (Col-0 × *ago4-3*). Analysis of the germination rate under optimal and stress conditions of the resultant F₂ lines showed a recovery of the wild-type phenotype in plants where wild-type AGO4 protein levels were detected (Figures 1d and S3). Additionally, the *ago4-3* null allele was introgressed into wild-type Col-0 plants (*ago4-3* × Col-0) and the resulting homozygous lines (F₂), where AGO4 protein was not detected by Western blot (Figure S3), showed high germination rates

under salt stress, similar to those shown by the *ago4* null mutants (Figure 1e), confirming that this phenotype resulted from the absence of AGO4. The germination rate of the crossed lines under optimal conditions showed no differences (Figure S1f,g).

The phenotypes of *ago4* mutants extend into seedling stages, with no significant effect when seedlings were grown under optimal conditions (Figure S5c,d). Seedlings carrying AGO4 null alleles showed longer primary roots when exposed to salinity compared with wild-type plants (Figure S5a,b), whereas the *ago4-2* mutant showed a detrimental effect on primary root length (Figure S5a). The phenotypic effects of these mutants are analogous to those observed during germination (Figure 1b,c).

AGO6 plays a role during germination under salinity when AGO4 is absent

The contrasting difference between AGO4 null and *ago4-2* mutant phenotypes led us to hypothesize that either AGO4 was playing an additional role, independent of the RdDM pathway during this plant developmental stage in response to stress, or that in the absence of AGO4, AGO6, expressed in low levels in the seed embryo (Havecker *et al.*, 2010), could play an unusual role under these conditions. To distinguish between these two possibilities, the phenotype of the *ago4-6 ago6-2* double mutant was analyzed during germination under the same stress conditions. The results showed that the double mutant germinates with a lower rate than the wild-type genotype under salinity, similar to that shown by the mutants lacking other core RdDM elements, whereas it showed a wild-type phenotype under optimal conditions (Figures 1a,f and S1h), and in sharp contrast to the higher germination rate shown by the different *ago4* null mutants (Figures 1c,f and S2). These data indicate that the *ago4* phenotype did not result from an additional AGO4 function but rather from the contribution of AGO6 in this plant response, perhaps by binding siRNAs that in the absence of AGO4 are preferentially associated with AGO6, producing a synthetic phenotype. In the absence of both AGO proteins, the plant stress response is compromised as in the case of the rest of the RdDM mutants tested causing a deficient germination (Figure 1a, f). This interpretation is supported by the null *ago6* single-mutant phenotype, which showed wild-type behavior under the conditions tested (Figure 1f), indicating that AGO6 by itself does not play a role in this process.

AGO4 protein abundance changes during germination and early seedling growth

Given the above evidence indicating that RdDM is needed for optimal germination under salinity stress, and the critical role assigned to AGO4 in this pathway, we asked whether its abundance is modulated during this process. For this, we tracked AGO4 protein accumulation during

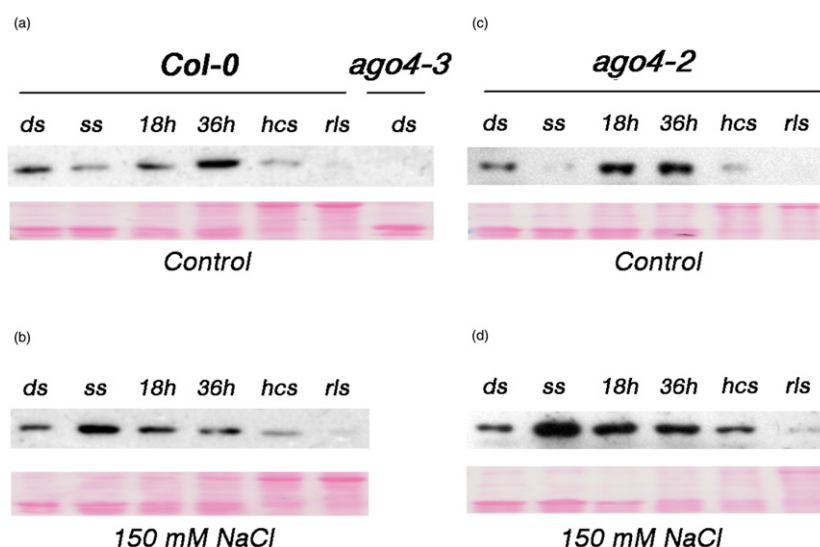
germination and throughout early seedling growth under optimal and salt-stress conditions. We performed Western blot assays using an AGO4-specific antibody against total protein extracts from six developmental stages: dry and stratified seeds, germinating seeds at 18 and 36 h, seedlings where hypocotyl and cotyledons have emerged from the seed coat, and seedlings with two rosette leaves, all germinated under optimal conditions. The results showed that the accumulated AGO4 protein present in dry seeds decreased after stratification, but then progressively increased until 36 h post-stratification, when its highest levels were achieved. After this time point, AGO4 protein levels gradually declined again until the last stage tested (Figure 2a). Under salinity conditions (150 mM NaCl), we found a markedly different AGO4 accumulation pattern, where the highest protein levels were detected in stratified seeds, with a subsequent gradual reduction, and with the lowest levels found in seedlings with two rosette leaves, as observed under non-stress conditions (Figure 2b). We did not detect changes in AGO4 transcript accumulation in response to salinity during germination (Figure S6), indicating that under these conditions AGO4 protein abundance is not controlled at the transcriptional level. It is worth mentioning that the accumulation patterns of the point mutant protein encoded by the *ago4-2* allele were similar to those found using wild-type seeds, indicating that AGO4-2 protein synthesis and stability are not drastically affected (Figure 2c,d). These data demonstrate not only that AGO4 is present during germination and early seedling growth, but also that its levels are modulated upon stress, in consonance with a functional role for the canonical RdDM pathway during these developmental stages and in response to adverse germination environments.

AGO4 is differentially localized in response to salinity

To explore in which seedling regions RdDM exerts its function during seed germination, we determined the tissue distribution of AGO4 during germination and early seedling growth stages. For this end we used transgenic plants containing a *GFP-AGO4* translational fusion under the control of the *AGO4* endogenous promoter (*pAGO4::GFP-AGO4*) expressed in a wild type background (Ye *et al.*, 2012). Protein localization was determined by GFP fluorescence using confocal microscopy of isolated embryos and young seedlings at different times after imbibition. As expected for AGO4, most of the fluorescence signal was localized in cell nuclei across the different tissues (Figure S7). GFP fluorescence showed a high AGO4 abundance and broad distribution in embryos imbibed for 8 h (Figure 3a). Remarkably, just after testa rupture the AGO4 distribution changed, maintaining its abundance in cotyledons but with lower levels and more dispersed localization observed in radicles. This distribution pattern was then maintained throughout radicle protrusion, late germination phase and young seedling growth (60 h after imbibition). At the later stage AGO4 accumulation was even lower in cotyledons, whereas the signal was detected in hypocotyls and root tips (Figure 3a).

When this analysis was performed on embryos and seedlings exposed to salt stress (100 mM NaCl), GFP fluorescence was also found in cotyledons and radicles; however, a strong signal was clearly detected in vascular tissues in both embryo regions (Figure 3b). This pattern was also present after testa rupture and was followed by a significant reduction during subsequent stages, with the fluorescence signal being barely detected in the roots or cotyledons of young seedlings.

Figure 2. ARGONAUTE 4 (AGO4) protein levels are modulated during germination and in response to stress. (a, c) Western blot immunodetection of AGO4 protein during germination and early seedling development from wild-type (*Col-0*), *ago4-3* and *ago4-2* seeds, germinated under optimal conditions; ds, dry seeds; ss, stratified seeds; 18 and 36 h (after stratification); hcs, seedlings with emerged hypocotyls and cotyledons; rls, seedlings with two rosette leaves) (upper row); Ponceau staining of the membranes used above, as loading reference (lower row). (b, d) As before, except that seeds were germinated in media containing 150 mM NaCl.



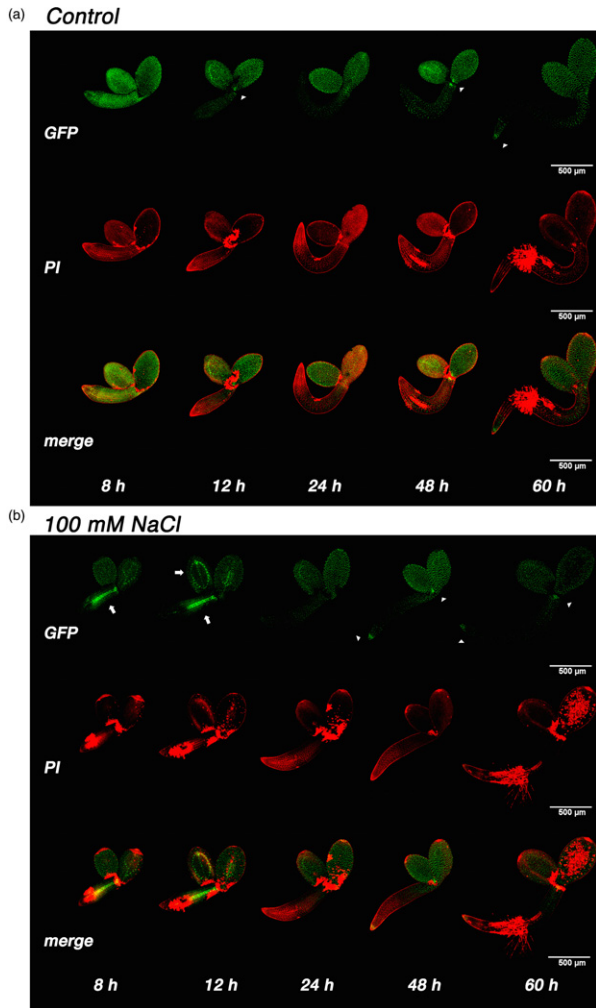


Figure 3. ARGONAUTE 4 (AGO4) shows differential tissue distribution during germination and early seedling development under optimal and high salt conditions. (a) GFP-AGO4 fluorescence detection in isolated embryos of 8, 12, 24, 48 and 60 h after imbibition (GFP, upper row); propidium iodide fluorescence of the same samples (PI, middle row); both signals merged (lower row). (b) Samples as described in (a), except that seeds were germinated in media supplemented with 100 mM NaCl. For detail, see Experimental procedures. These images are representative samples of at least eight individuals analyzed per experiment, and these observations were reproduced in four independent experiments. Arrowheads and arrows indicate apical and root meristematic regions, and vascular tissues showing high AGO4 abundance, respectively.

We noticed that during late germination stages and early seedling growth a sharp signal could be detected in shoot apical regions and in root tips (Figures 3a,b, and S8, arrowheads), consistent with previous findings by other groups using transcriptomic data obtained from roots of seedlings growing under optimal conditions (Kawakatsu *et al.*, 2016). This result strongly suggests that the canonical RdDM pathway plays a particular role in response to salinity during seed germination.

RdDM controls CHH methylation during germination under salinity in a locus-specific manner

To obtain a mechanistic insight into the role of the canonical RdDM in the plant response to salinity, we explored the DNA methylation differences between RdDM-defective (*ago4-3*, *ago4-2* and *nrpe1-11*, a Pol V null mutant) and wild-type lines germinated under optimal or high-salinity conditions by performing WGBS. As we anticipated, according to the proposed RdDM mechanism, no strong differences were found in terms of the global proportion of methylated cytosines on any of the three different methylation contexts found in plants (CG, CHG and CHH) in the mutant alleles, when compared with the wild type (Figure S9a). The distribution of CHH methylation was slightly decreased in the chromosome arms without noticeable changes in the centromeric regions, whereas the other methylation contexts (CG and CHG) remained unaffected (Figure S9b). These results are consistent with the activity and distribution previously reported for RdDM in terms of global DNA methylation (Schoft *et al.*, 2009; Wierzbicki *et al.*, 2012; Zhang and Zhu, 2012; Yaari *et al.*, 2019). Moreover, we did not notice any prominent effect as result of the salinity treatment over the global DNA methylation or its distribution along chromosomes in the wild type or in RdDM mutants (Figure S9a,b). Overall, these results suggest that RdDM does not produce a widespread effect at the genome level, but rather that it acts in a locus-specific manner in response to salinity during germination, similar to its activity in other developmental stages.

To validate the latter hypothesis, we identified differentially methylated regions (DMRs, defined as >10% methylation change in each mutant, compared with Col-0, with $P < 0.01$, adjusted for false discovery rate, in 100-bp sliding windows from the two biological replicates; see Experimental procedures) for each set of growth conditions. This analysis showed 191, 2597 and 1481 CHH hypomethylated DMRs in *ago4-2*, *ago4-3* and *nrpe1*, respectively. This number was nearly doubled in the AGO4 mutants and was increased by 20% in *nrpe1* when seeds were exposed to salinity (Figure 4a; Table S1), strongly supporting an active locus-specific role of the RdDM pathway during germination in response to salt stress. Interestingly, we also observed changes in the number of CG and CHG DMRs, in agreement with the participation of RdDM in the maintenance of DNA methylation (Law and Jacobsen, 2010). An overlapping analysis between the DMRs identified and the genomic features (see Experimental procedures) showed, as expected, that most of the DMRs are located within transposable elements (TE genes and fragments; Figure S10a), and that <20% were located in protein-coding genes (including up to 2 Kb of their regulatory regions), non-coding genes or pseudogenes, confirming that the main role of RdDM is to control the methylation of TEs.

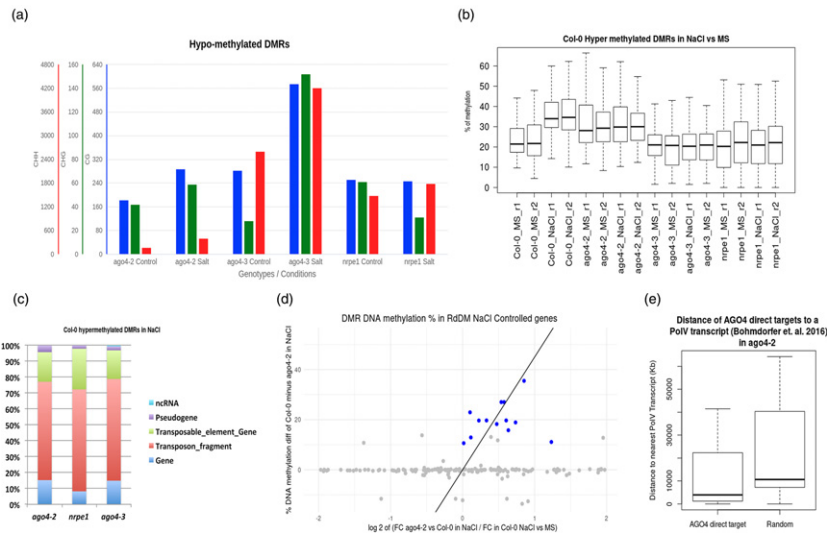


Figure 4. RNA-directed DNA methylation (RdDM) is required for the repression of a small subset of genes in response to salinity (a) Comparison between the numbers of hypomethylated differentially methylated regions (DMRs) identified in all of the genotypes and conditions tested in the Col-0 background. The y-axes show the number of hypo-DMRs in each methylation context. The precise values for each case are shown in Table S1. (b) RdDM dependence on the number of hypermethylated DMRs in wild-type seeds subjected to salinity treatments. Methylation is represented as a percentage for each genotype/treatment ($n = 170$). (c) Genomic features of the RdDM-dependent Col-0 DMRs in NaCl affected in each of the RdDM mutants (<10% of CHH methylation compared with Col-0 NaCl). Bars represent percentages of the total number of features mentioned in the text. (d) Correlation analysis of the salinity-dependent hypermethylated genes found in *ago4-2* and its transcriptional release from the repressive status imposed by NaCl in RdDM-deficient plants (blue dots). Gray dots represent a random subset ($n = 200$) of genes, with methylation status on its promoter region and transcriptional status shown as a control. (e) Distance to the nearest Pol V transcript with the selected subset of genes in (d) compared with the same number of random regions with the same length ($n = 13$).

RdDM can also affect protein-coding genes during germination under the conditions tested, however.

The *ago4-2* allele produces a low-activity AGO4 protein

As *ago4-2* was considered to be a dominant-negative AGO4 allele encoding a defective protein (Agorio and Vera, 2007), we expected a similar effect on methylation in *ago4-2* as in the null mutant (*ago4-3*). DMRs in *ago4-3* showed 10 times more hypomethylated CHH regions compared with *ago4-2* (Figure 4a; Table S1), however, suggesting that *ago4-2* produces an AGO4 weak allele. To investigate this possibility further, we performed an overlapping analysis of the DMRs identified in both mutants, under optimal and salinity conditions, and classified them into three sets: specific to *ago4-2*, specific to *ago4-3* or common to both. Under control conditions, we found 73, 2479 and 118 DMRs in these three sets, respectively. With NaCl treatment we found 179, 3985 and 221 DMRs in the three respective sets. Thus, in both conditions, about 60% of *ago4-2* DMRs are common with *ago4-3* (Figure S10b). We then looked at the methylation effects in DMR sets specific to *ago4-2* (Figure S10c,d) and to *ago4-3* (Figure S10e,f) in the different genetic backgrounds. The results showed that specific *ago4-2* DMRs present lower methylation than wild-type DMRs in *ago4-3* and *nrpe1* genotypes under both

conditions (Figure S10c,d), a reduction that was not detected before because it was lower than the cut-off value considered to define a DMR (10%, see Experimental procedures). When we looked at the methylation level of the specific *ago4-3* DMRs in *ago4-2*, we found that it was similar to that in the wild type, whereas in *nrpe1* it was low, as in *ago4-3* (Figure S10e,f). Therefore, these data indicate that the *ago4-2* allele encodes an AGO4 protein with lower influence on methylation levels than observed in the wild type, but not as reduced as in AGO4 or Pol V null mutants, consistent with an AGO4 weak allele. Despite the residual activity of the *ago4-2* allele in terms of DNA methylation, its phenotype is clearly similar to *nrpe1* and to other RdDM core element null mutants (Figure 1a,b), indicating that, even though the DNA methylation effect in *ago4-2* is not as penetrant as in *nrpe1*, it is sufficient to alter the RdDM impact on germination under salinity.

The RdDM pathway controls locus-specific methylation in response to salinity during germination

To identify AGO4-dependent methylated regions, we looked for wild-type (Col-0) DMRs that gain CHH methylation under salinity stress. This analysis identified 170 DMRs with higher methylation by comparing stress vs non-stress in wild type seeds. To determine whether AGO4

was participating in the methylation of such regions in response to salinity, we compared their methylation profiles in *ago4-2* and *ago4-3* mutants grown in optimal and salinity conditions using the *nrpe1* methylation profile as the RdDM reference. The comparison of the methylation gain between non-stress and stress conditions showed differences for the wild-type line, as expected, but not for *nrpe1*, *ago4-2* and *ago4-3*. As anticipated for an AGO4 weak allele, *ago4-2* showed a small methylation decrease compared with *ago4-3* (Figure 4b). These results indicate that most of the locus-specific changes in CHH methylation in response to this stress depend on AGO4 and the RdDM activity.

Analysis of the genomic features of the DMRs exhibiting the strongest reduction in DNA methylation (>10%), when Col-0 was compared with *ago4-2* (20 regions), *nrpe1* (64 regions) or *ago4-3* (127 regions), showed that most of them correspond to TE genes and TE fragments, typical targets of the canonical RdDM (Figure 4c).

RdDM participates in the control of germination timing

To obtain information on the impact of AGO4 on gene expression during germination under salinity conditions, we performed RNA-seq experiments using Col-0, *ago4-3* and *ago4-2* seedlings germinated under optimal and salinity conditions. We first focused on the hypermethylated regions previously identified in Col-0 from salinity conditions that also showed lower DNA methylation levels in *ago4-2* (170 DMRs, see Figure 4b). We searched for protein-coding genes containing these regions, as well as for those falling within 5 kb on each side of the recognized TEs (Figure 4c). Out of 78 potential target genes, we identified a subset of 13 genes for which expression is lower in Col-0 in response to salt but is higher in *ago4-2*, consistent with the higher CHH methylation occurring nearby in wild-type genotypes (Figure 4d; Table 1). Hence, this result suggests that the RdDM-dependent CHH methylation deposition is responsible for the lower expression of these genes during germination under salinity, and that this repression is released in the absence of a functional AGO4/RdDM. In accordance with this outcome, these genes are located significantly closer to previously identified Pol V target sites, when compared with a set of randomly selected regions (Bohmdorfer *et al.*, 2016) (Figure 4e). Consequently, this set of RdDM-regulated genes might be at least partially responsible for the *ago4-2* germination phenotype observed under salt stress (Figure 1b).

Most of the genes identified (8/13) from this analysis are related to signal transduction or other regulatory functions, some of which have been involved in the control of dormancy and/or germination or in functions related to these processes (Table 2). Among them, EIN3 BINDING F-BOX1 (*EBF1*), encoding a component of the Ub-protein ligase (E3) that, together with *EBF2*, is essential for proper

Table 1 RdDM target candidate list with a corresponding change in DNA methylation found in *ago4-2*

Targets found in <i>ago4-2</i>			
AGI ^b	Deregulation in <i>ago4-2</i> ^a	DNA methylation difference ^c	Name
AT2G05786 ^d	3.23818	12.4681	hypothetical protein
AT5G35830 ^d	2.28452	11.8333	Ankyrin repeat family protein
AT3G25490 ^d	1.23218	11.0896	Protein kinase family protein
AT3G15300 ^d	0.734898	18.8961	VQ motif-containing protein
AT3G28940 ^d	0.635058	15.7812	ALG2-like (avirulence induced gene) family protein
AT5G37670 ^d	0.604745	19.6897	HSP20-like chaperones superfamily protein
AT3G26470 ^d	0.576367	27.0098	Powdery mildew resistance protein, RPW8 domain
AT3G26480 ^d	0.536978	27.0098	Transducin family protein/ WD-40 repeat family protein
AT5G52070 ^d	0.474015	18.2488	Agenet domain-containing protein
AT5G37660 ^d	0.331682	19.6897	plasmodesmata-located protein
AT1G41830 ^d	0.225374	19.6587	SKU5-similar 6
AT5G07680	0.114474	12.8979	NAC domain containing protein
AT2G19830 ^d	0.0149694	10.619	SNF7 family protein

^aDeregulation is represented as follows: $\log_2((FC\ ago4-2\ NaCl\ versus\ Col-0\ NaCl)/(FC\ Col-0\ NaCl\ versus\ Col-0\ MS))$.

^bOnly targets with repression in Col-0 NaCl versus Col-0 MS were selected.

^cDNA methylation difference is the percentage result from: $(ago4-2\ NaCl - (Col-0\ NaCl - Col-0\ MS)) / (Col-0\ NaCl - Col-0\ MS) \times 100$ CHH DNA methylation.

^dTarget is also found in *ago4-3*.

ethylene signaling (Binder *et al.*, 2007), underscores the control of seed dormancy through the ethylene-DOG1 pathway under stress conditions (Nishimura *et al.*, 2018; Li *et al.*, 2019). It is also worth noting the *NAC4* gene transcription factor, the expression of which is regulated by AFB3 (Vidal *et al.*, 2014; Lee *et al.*, 2017), an auxin receptor involved in various aspects of plant development, including the auxin-mediated control of seed dormancy (Liu *et al.*, 2013).

When we performed the same analysis with the *ago4-3* null mutant we found a subset of 18 out of 83 candidate genes, the expression of which under salt treatment in Col-0 is derepressed in this mutant, consistent with the loss of CHH methylation on the nearby DMRs (Figure S11a) and their relative proximity to a Pol V transcribed region

(Bohmdorfer *et al.*, 2016) (Figure S11b). Twelve of these targets are shared with *ago4-2* (Table S2), indicating that they are *bona fide* AGO4/RdDM direct gene targets. Additional targets in this mutant could be a consequence of the complete loss of AGO4 activity and/or AGO6 interference, as demonstrated in the previous sections.

Beyond the direct targets, the phenotype of RdDM mutants should involve the deregulation of many downstream genes. To characterize these broader effects of AGO4/RdDM during germination, and in response to salinity, we analyzed the differential accumulation of transcripts in *ago4-2*, *ago4-3* and wild-type lines. We found that transcript accumulation profiles overall are similar between wild type and *ago4-3* lines, and slightly different to *ago4-2* (Figure S12a–c). Interestingly, differences were also found between wild type and the mutants even under optimal growth conditions (Figure S12a). This shows that although RdDM mutants have no detectable phenotype during germination in the absence of salt stress, they still have some transcriptional effects (Figure S1).

To identify the differentially accumulated transcripts under stress conditions between wild-type, *ago4-2* and *ago4-3* lines, we performed a correlation analysis (Figure S12b,c) and selected outliers as genes strongly upregulated or downregulated by salt in the mutants. As we anticipated, many genes are shared by the *ago4-2* and the *ago4-3* subsets (Figure S12d,e). The greater differences in abundance were found among transcripts associated with seed maturation, dormancy and germination (Figure 5a; Tables S3–S6), with most of them related to metabolic functions. Comparison analysis between *ago4-3* and wild-type expression patterns during germination under salt stress highlights the upregulation of transcripts involved in dormancy, germination and growth in *ago4-3* (Figure 5a),

consistent with the higher germination rate of this line. This is also the case for transcripts encoding two 2C-type protein phosphatases (AHG1 and AHG3), proteins that are known to interact with DOG1, an ABA-independent key regulator of seed germination (Nishimura *et al.*, 2007; Nee *et al.*, 2017; Li *et al.*, 2019), as well as the transcript encoding ILITHYA (ILA), a protein that mediates the phosphorylation of eIF2 α by the activation of GCN2, and hence is involved in the modulation of translation under stress recovery (Faus *et al.*, 2018). Also, transcripts involved in growth and metabolism, such as ribosomal proteins, sucrose synthase, phosphofructokinase and stay-green protein, an SnRK1 subunit implicated in the regulation of carbon metabolism, among others, are upregulated (Table S3). The same analysis using *ago4-2* showed that the transcript encoding AHG1 was among the upregulated transcripts, indicating that the AGO4/RdDM pathway indirectly modulates its transcription. In addition, other notable upregulated transcripts encode for various late embryogenesis abundant proteins and for the ANAC032 transcription factor, involved in photosynthesis inhibition and the reprogramming of carbon and nitrogen metabolism (Sun *et al.*, 2019), processes that might be related to delayed germination (Table S5).

DISCUSSION

Although most of the information on the regulatory roles of the RdDM pathway has been analyzed during reproductive processes (Matzke and Mosher, 2014; Matzke *et al.*, 2015), there are a few examples where the contribution of this pathway in the plant response to abiotic stress has been investigated (Ito *et al.*, 2011; Matsunaga *et al.*, 2012; Tricker *et al.*, 2012; Popova *et al.*, 2013; Chan *et al.*, 2016). In this last case, the control of transposable elements has

Table 2 Proposed ARGONAUTE 4 (AGO4)/RNA-directed DNA methylation (RdDM) targets and their functions

AGI	Name	Description	Function	References
At2g25490	EBF1	Ub-protein ligase E3	Essential for proper ethylene perception together with EBF2	Binder <i>et al.</i> , 2007
At2g19830	VPS32 or SNF7.2	SFN7-domain protein	Involved in vacuolar protein sorting, and component of the ESCORT complex	Winter and Hauser, 2006; Gao <i>et al.</i> , 2017
At5g35830	At5g35830	Ankikin-repeat family protein	Implicated in targeting cytosol proteins to organellar outer membranes	Becerra <i>et al.</i> , 2004; Gissot <i>et al.</i> , 2006
At5g37660	PDLP7	Plasmodesmata-located protein 7	Protein containing two DUF26 motifs and implicated in bacterial immunity	Thomas <i>et al.</i> , 2008; Aung <i>et al.</i> , 2019
At5g52070	At5g52070	Agenet domain-containing protein	Associated with chromatin remodeling with significant impact on gene expression. It has been proposed as an RdDM target	Maurer-Stroh <i>et al.</i> , 2003; Kurihara <i>et al.</i> , 2008
At3g15300	MVQP	VQ motif-containing protein	This protein is phosphorylated by MAPKs and interacts with WRKY transcription factors	Cheng <i>et al.</i> , 2012; Jing and Lin, 2015
At5g07680	NAC4	NAC domain-containing protein	Its transcript is targeted by miR164 and its expression is regulated by AFB3, an auxin receptor	Vidal <i>et al.</i> , 2013; Lee <i>et al.</i> , 2017
At1g41830	SKS6	SKU-similar 6	A multi-copper oxidase-like protein involved in cotyledon vascular patterning	Jacobs and Roe, 2005

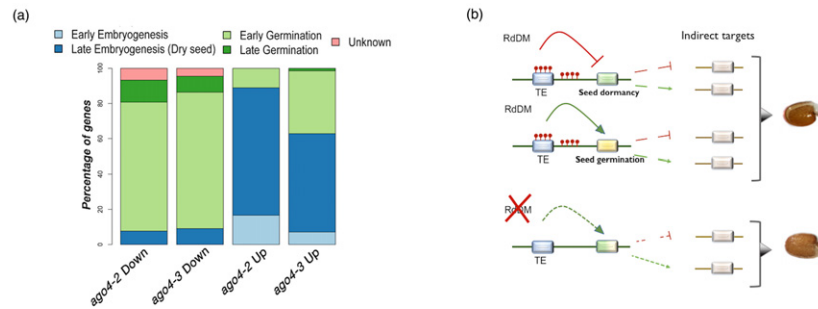


Figure 5. RNA-directed DNA methylation (RdDM)-dependent ARGONAUTE 4 (AGO4) activity participates in the control of the germination process. (a) Proportion of salt-responsive transcripts in *ago4-2* and *ago4-3* lines (Tables S3–S6). The classification into early and late embryogenesis (seed maturation) and early and late germination (initial growth processes and post-germination growth, respectively) categories was made considering the highest expression peak for every gene in the analysis. (b) Proposed model for RdDM participation in the control of the germination process in response to adverse environments: in wild-type seeds, under stress conditions, the canonical RdDM pathway controls the germination process by favoring or repressing the expression of genes needed for its initiation and/or progression. This control is exerted through DNA methylation (red dots) of its canonical target regions (transposable elements, blue boxes) that neighbor the controlled genes; those genes may be key modulators of the germination process through the control of a broad transcriptional network (indirect targets). When the RdDM is lost this regulation is eliminated, affecting the appropriate response to stress during germination.

been described as one of the mechanisms regulating the transcription of a diversity of genes (Secco *et al.*, 2015; Au *et al.*, 2017), but only a small number of target genes have been identified (Kurihara *et al.*, 2008; Au *et al.*, 2017; Iwasaki *et al.*, 2019). Recently, it has been reported that non-canonical RdDM participates in the maternal control of Arabidopsis seed dormancy, as well as in the enhanced dormancy produced by cold during seed development (Iwasaki *et al.*, 2019). In this work, we addressed the involvement of the canonical RdDM pathway in the regulation of the plant response to abiotic stress imposed by salinity during germination, a critical developmental stage during the plant life cycle.

Our results showed that mutants affected in different canonical RdDM core elements exhibit delayed germination under salinity, demonstrating that this pathway participates in the modulation of the germination process in high-salt environments. Although RdDM has been implicated in the plant response to environmental stresses under other circumstances, our results show that it also plays an important role in the decision to germinate, a requirement for optimal adjustment in plants grown under stress.

Unexpectedly, the analysis of seeds lacking AGO4 (*ago4-3*) showed contrasting behavior, displaying a higher germination rate than wild-type seeds under stress conditions. This observation was further investigated showing that this phenotype is not the result of an additional RdDM-independent AGO4 function but instead is linked to the action of the AGO6 protein. These data lead us to propose that, under these conditions, when AGO4 is not available AGO6 is able to bind otherwise AGO4-specific siRNAs. As the AGO6 or AGO9 transcript levels do not change in the AGO4 mutants used (Figure S6), and given the AGO6 distribution reported in Arabidopsis seeds (Havecker *et al.*,

2010; Eun *et al.*, 2011), it is possible to predict that AGO6 would not be able to fully compensate for the absence of AGO4, therefore leading to a synthetic phenotype. The action of AGO6 was not detected in the *ago4-2* mutant, however. A plausible explanation for this outcome is that the defective AGO4 protein produced by this weak allele still efficiently binds siRNAs, and thus such siRNAs are not available for apocryphal AGO6 binding.

Consonant with the involvement of RdDM in the germination process in a non-stress environment (this work; Kawakatsu *et al.*, 2017), high AGO4 protein levels were detected in dry seeds, which change throughout germination and post-germination. The AGO4 tissue localization also changes throughout these periods, and in some stages the protein is also localized in root meristematic regions. The AGO4 post-germination distribution, where AGO4 levels decrease in radicles and do not change in cotyledons, are consistent with its participation during those stages, when seedlings have to confront their transition to a different environment.

Germination in the presence of high salt concentrations leads to a drastic change in AGO4 distribution; in particular, AGO4 becomes highly abundant in the radicle vascular cylinder, and with less intensity but clearly patent in cotyledon vasculature. Under both germination conditions it is observed that AGO4 protein levels decrease in the roots, whereas they do not change much in cotyledons through the post-germination stages and continue to be present in the meristematic regions up to the latest periods tested. Although at this point we do not have enough data to explain this remarkable shift in AGO4 allocation towards vascular tissues, it is likely that this is a response to the severe stress conditions occurring around vascular cells, where salt is transported once it is taken up from the

growth medium. The finding of AGO4 and other RdDM component transcripts in the root stele supports the distribution observed (Kawakatsu *et al.*, 2016). These results point to a possible RdDM regulatory role in the vascular system in response to stress, and/or in a long-distance communication strategy for alarm, as suggested by siRNA transport to neighboring cells, or to a potential translocation through the phloem (Melnik *et al.*, 2011; Sarkies and Miska, 2014).

As expected, seed germination under high salt concentrations produced different changes in transcript abundance profiles between all lines, when they are compared with those obtained from non-stress conditions. Not all of them share transcripts involved in protection against salt stress, however, indicating that the difference in germination rates is not necessarily linked only with salt defense responses. It is noteworthy that differences were found when CHH DNA methylation patterns arising from salinity were compared between the wild type and the *ago4-2* and *ago4-3* lines. Of special interest are genes showing lower methylation levels in *ago4-2* and *ago4-3* than in wild type, presenting genomic features characteristic of RdDM targets (neighboring to a TE) and their closeness to Pol V transcripts (Bohmdorfer *et al.*, 2016). Most of these genes are shared between the two AGO4 mutants; hence, corroborating their methylation dependence on the RdDM pathway, which prevents their transcriptional activation under salinity conditions. Although not many protein-coding gene targets were found in this analysis, this outcome is consistent with previous reports showing a small contribution of RdDM-dependent repressive marks on gene expression (Zheng *et al.*, 2013; Gallego-Bartolome *et al.*, 2019).

The majority of the identified genes with these characteristics encode proteins that have been associated with different regulatory roles during germination. *EBF1* (At2g25490) is of particular interest because it encodes a nuclear F-Box protein component of a Ub-protein ligase (E3) that targets EIN3 for degradation, a key transcription factor playing a positive role in ethylene perception. Deficiency of *EBF1* leads to an increase in EIN3 levels inducing hypersensitivity to ethylene (Binder *et al.*, 2007; Merchante *et al.*, 2013), a plant hormone that plays a pivotal role in the control of dormancy and germination (Corbineau *et al.*, 2014). In *Arabidopsis* and in numerous other species, ethylene promotes the germination of non-dormant seeds under diverse adverse environments, including conditions of high salinity (Wang *et al.*, 2007; Lin *et al.*, 2013), and interestingly enough the disruption of the ethylene signaling pathway leads to salinity and osmotic stress sensitivity during germination (Leubner-Metzger *et al.*, 1998; Pirrello *et al.*, 2006). These observations are in consonance with our findings showing that defective CHH DNA methylation in the *ago4-2* mutant during germination under conditions of salinity results in the upregulation of *EBF1* (compared

with the wild type), which would have a negative effect on ethylene perception, and as a consequence would lead to a lower rate and/or capacity of germination. Despite a similar effect on *EBF1* expression and methylation for *ago4-3*, the effect on germination was contrasting, suggesting that the activity of AGO6 in the AGO4 null mutant counteracts *EBF1* downstream effects. Further experimentation is needed to establish whether some of the genes in which DNA methylation is affected in *ago4-2* also participate in the signal transduction pathways related to ethylene function, and/or in pathways involved with other hormones with recognized roles in dormancy and germination, such as abscisic acid (ABA) and gibberellic acid, the signaling pathways of which have close communication with the signaling pathway for ethylene (Corbineau *et al.*, 2014).

As the high abundance of AGO4 in root and cotyledon vascular tissues in response to salinity suggests systemic translocation, it is worth highlighting the *PDLP7* gene (At5g37660), the product of which is a plasmodesmata-located protein (PDL) involved in cell-to-cell communication (Thomas *et al.*, 2008), and *SKS6* (At1g41830), upregulated by ABA and encoding a multi-copper oxidase-like protein that participates in cotyledon vascular patterning in *Arabidopsis* (Jacobs and Roe, 2005).

The participation of the AGO4/RdDM pathway in germination under salinity demonstrated by the RdDM mutant phenotypes is strengthened by the transcriptomic profiles obtained from the RNA-seq analysis, as the comparison with wild-type expression patterns exhibited differential accumulation levels for transcripts mostly implicated in dormancy, germination and post-germination processes. For *ago4-2*, showing low germination rate and capacity, like the rest of the RdDM mutants, some mRNAs that typically accumulated in mature embryos (LEA and storage proteins) stand out among the upregulated transcripts, as well as an mRNA encoding a stress-responsive transcription factor (ANAC032) induced by carbon starvation and involved in the inhibition of photosynthesis, and in the regulation of carbon metabolism, nitrogen assimilation and amino acid catabolism (Sun *et al.*, 2019). Also, consistent with the *ago4-2* phenotype, the AHG1 transcript showed higher levels than the wild type upon salinity treatment. AHG1 is a type-2C protein phosphatase (PP2C), usually highly abundant during seed maturation, that together with DELAY OF GERMINATION 1 (DOG1) control seed dormancy and germination, independently of ABA (Nee *et al.*, 2017; Nishimura *et al.*, 2018). Recently, it has been shown that ethylene partially controls seed dormancy/germination through the DOG1 pathway (Li *et al.*, 2019), in agreement with our finding that RdDM-dependent methylation might control *EBF1* expression, a participant of ethylene signal transduction.

Among the upregulated transcripts in *ago4-3*, we found two encoding PP2C proteins involved in the regulation of

seed dormancy and germination, AHG1 and AHG3. These PP2C phosphatases seem to have overlapping and distinctive functions, showing similar activities but different spatial and temporal expression patterns (Nishimura *et al.*, 2007, 2018); however, ABA receptor transcripts were not detected among the differentially expressed mRNAs, suggesting that at least a pool of AHG1 and AHG3 phosphatases could be in their active forms, as expected for germinating seeds (Cutler *et al.*, 2010). Furthermore, in agreement with its higher germination rate under salinity conditions, we identified a higher abundance of transcripts involved in active growth and metabolism than in wild-type seeds.

As a whole, the methylome and transcriptome data in this work exhibit the role of the AGO4/RdDM pathway in germination and dormancy processes; particularly, by modulating the germination timing, a function that is more evident under stressful environments (Figure 5b). Also, the resultant information exposes the complexity of the gene expression changes affecting numerous gene networks, leading to the characterized phenotypes. It should be noted that we did not detect any effect on germination rate and capacity when the mutant seeds affected in different core RdDM elements were exposed to optimal growth conditions, showing that any effect of RdDM on *A. thaliana* seed development (Wang and Köhler, 2017; Kirkbride *et al.*, 2019; Chow *et al.*, 2020) does not impact the germination process.

Even though further experimentation is needed to understand the precise role of the RdDM pathway activity in Arabidopsis seed germination and dormancy in response to salt stress, the findings in this work unveil RdDM gene targets, some of which have been previously involved in signaling pathways controlling germination timing, and others that prompt new questions regarding the control mechanisms involved in the plant responses to salinity, providing a state-of-the-art potential source for the search of targets for improving future farming on salt-affected soils.

EXPERIMENTAL PROCEDURES

Plant material and growth conditions

In this work we used seeds of *A. thaliana* (L.). For propagation or germination experiments, seeds were surface sterilized with absolute ethanol for 2 min, washed with 40% commercial bleach containing 0.02% Triton X-100 (Sigma-Aldrich, <https://www.sigmaaldrich.com>) for 8 min, and were rinsed five times with sterile milliQ[®] water. After sowing, seeds were stratified on MS plates for 2 days (for Columbia) or 4 days (for *Ler* and *Ws*) in the dark at 4°C and then transferred to optimal growth conditions in a growth chamber held at 21°C and 40–60% relative humidity, with a 16-h light/8-h dark photoperiod under white light (80–100 $\mu\text{mol m}^{-2} \text{sec}^{-1}$). Seeds were germinated in round dishes containing full-strength MS salts (4.3 g L⁻¹, with macro- and micronutrients, without vitamins; Caisson Labs, <https://caissonlabs.com>), 1% sucrose

(Research Organics, <https://resorg.lookchem.com>), 0.5 g L⁻¹ 2-(*N*-morpholine)-ethanesulphonic acid (MES; Calbiochem, now Merck, <https://www.merckmillipore.com>) and 0.65% agar (Sigma-Aldrich). For propagation, 2-week-old seedlings were transferred (or directly sown) into soil (Metromix 200; Hummert International, <https://www.hummert.com>) and kept under the described growth conditions with optimal watering until the siliques were dry.

Mutant lines *nprpd1-1*, *nrpe1-11*, *rdr2-1*, *dcl3-1* and *ago4-6* in the Col-0 background, and *ago4-1* in the *Ler* background (Zilberman *et al.*, 2003), were obtained from ABRC (<https://abrc.osu.edu>) or NASC (<http://arabidopsis.info>), whereas *ago4-2*, *ago4-4* and *ago4-3*, in the Col-0 background, were kindly donated by Pablo Vera (Agorio and Vera, 2007), Michael Axtell (Wang and Axtell, 2017) and Blake Meyers, respectively. The seeds of the double mutant *ago4 ago6* were kindly donated by J-K Zhu (Duan *et al.*, 2015). For genetic crosses, plants were grown in the conditions described above until the first floral buds were visible. Crossed flowers were marked and plants were grown under optimal conditions as described until seeds were dry. Offspring from introgressed lines and crosses were identified by marker selection and by PCR.

Germination under optimal and stress conditions

Seeds used for germination experiments were collected from plants growing under optimal conditions until senescence. Harvested seeds were stored under low humidity at 4°C for at least 2 weeks before use. Germination under salt conditions was achieved in MS media supplemented with 100–250 mM NaCl (JT Baker, now Fisher Science, <https://www.fishersci.com>), as indicated. Germination was quantified by radicle emergence from five technical replicates of 50 seeds each. All germination experiments were performed with seeds of the same age and were replicated at least five times.

Root length determination

For root length experiments, stratified seeds were sown in square 10 × 10 cm vertical dishes containing 0.2× MS salts, 1% sucrose and 1% agar or in medium containing 100 mM NaCl. After sowing, plants were grown under the conditions described above. After radicle protrusion, root length was measured by marking the root tip position of every plant every day at the same hour until day 8. The measurements were made using IMAGEJ[®] (<https://imagej.nih.gov/ij>).

Statistics applied to phenotypic analyses

The germination experiments included in this work were replicated five times using 50 seeds per replicate and five biological replicates. Data were accumulated over time and fitted to sigmoidal dose–response curves with variable slope: $y = \text{bottom} + (\text{top} - \text{bottom}) / (1 + 10^{((\text{LogEC50} - x) \times \text{hillslope})})$, also called the four-parameter logistic equation. ‘Bottom’ is the y value at the lower plateau (constrained to zero), ‘top’ is the y value at the upper plateau, ‘LogEC50’ is the x value when the response is half-way between the bottom and the top and ‘hillslope’ describes the steepness of the curve. The null hypothesis was that two curve-fitting parameters (hillslope and LogEC50) from each data set were the same (Olvera-Carrillo *et al.*, 2010).

For root-length experiments, length was measured every day ($n = 15$ for optimal conditions and $n = 60$ for salinity conditions) with three biological replicates; data were accumulated over time and fitted to sigmoidal dose–response curves with variable slope, as described above.

Protein extraction and Western blot assays

Total protein extracts from seedlings, dry seeds or germinating seeds were obtained according to the method described by Olvera-Carrillo *et al.* (2010). Protein contents were quantified by the Lowry protocol (Lowry *et al.*, 1951) and separated in 10% sodium dodecyl sulphate polyacrylamide gel electrophoresis (SDS-PAGE). Western blots were performed following standard protocols using 30–40 µg of protein extracts. Anti-AGO4 antibody (Agriseria, <https://www.agrisera.com>) was used in 1:2000 to 1:4000 dilutions, whereas secondary antibody (anti-rabbit horseradish peroxidase; Zymed, now ThermoFisher Scientific, <https://www.thermofisher.com>) was used in 1:20000 or 1:30000 dilutions. Signals were developed with peroxidase substrate from Supersignal West Pico (ThermoFisher Scientific) and exposed to blue X-ray films (Kodak, <https://www.kodak.com>). Films were photographed using IMAGEQUANT 300 (GE Healthcare, <https://www.gehealthcare.com>).

Fluorescence microscopy

For these experiments, we used seeds from *pAGO4::GFP-AGO4* transgenic Arabidopsis that were kindly donated by Dr Qi (Ye *et al.*, 2012). This construction allows the production of a chimeric AGO4 wild-type protein fused at its N terminal with GFP under the control of the native *AGO4* promoter. Seeds were germinated in plates containing full-strength MS medium or full-strength MS medium supplemented with 100 mM NaCl. Whole embryos were isolated under the microscope and immediately stained with 20 µg µl⁻¹ propidium iodide (Sigma-Aldrich) for 20 min and observed using an Olympus FV1000 upright confocal microscope (Olympus, <https://www.olympus-global.com>) with a 10× objective. Embryo images were obtained from stacks of individual digital slices with a thickness of 6.23 µm. In the case of the intracellular analysis, a 60× objective was used, and images were obtained from stacks of individual digital slices (500 pixel × 456 pixel), with a thickness of 0.8 µm. GFP and propidium iodide were excited at 488 and 568 nm, respectively. Fluorescence brightness in the GFP channel was increased with IMAGEJ without affecting signal distribution.

RNA isolation and high-throughput sequencing

Total RNA from germinated seeds was extracted using the hot phenol method (Mylne *et al.*, 2010). For high-throughput sequencing analysis, RNA was obtained from the wild type and from *ago4-3* and *ago4-2* lines germinated in full-strength MS or full-strength MS supplemented with 100 mM NaCl. To achieve the most homogeneous representation of the different developmental stages for each line, samples were harvested when each seed population reached 50% germination in every condition examined. RNA-seq libraries were prepared from high-quality RNA, verified using a Bioanalyzer 2100 (Agilent, <https://www.agilent.com>). Construction of polyA RNA libraries was carried out using the TrueSeq stranded mRNA Library Prep kit (Illumina, <https://www.illumina.com>). High-throughput sequencing was performed on duplicate biological samples using the multiplex paired-end 2 × 75 configuration. Libraries and sequencing were performed by the Unidad Universitaria de Secuenciación Masiva de DNA (IBT-UNAM) with a HiSeq 2500 platform (Illumina).

RNA-seq analysis

For RNA-seq analysis, all libraries contained between 20.5 and 49.2 million high-quality reads per library with non-over-represented sequences. The obtained reads were aligned to the TAIR10

reference genome (<https://www.arabidopsis.org>) using SMALT 0.7.6 (Genome Research Ltd., <https://www.sanger.ac.uk>), and at least 99.74% of reads mapped to the genome. Hit counting was performed using SAMTOOLS (Li *et al.*, 2009). Differential expression analysis of RdDM direct targets were performed using EDGER (Robinson and Smyth, 2008).

To select and sort the genes in which repression in salt could depend on RdDM methylation (RdDM direct targets), we used a 'deregulation' score, with the following logic. Genes normally 'repressed' by RdDM in salt conditions should have a negative log₂('FC Col-0 NaCl versus Col-0 MS'). If they become 'de-repressed' by the lack of RdDM, they should have a positive log₂('FC *ago4* NaCl versus Col-0 NaCl'). The 'deregulation' value captures the effect of both conditions by subtracting the 'repression' term from the 'de-repression' term as follows: log₂('FC *ago4* NaCl versus Col-0 NaCl')/log₂('FC Col-0 NaCl versus Col-0 MS'). This applies only to genes that meet the 'repression' condition; genes with the highest 'deregulation' score are reported on Table 1 (*ago4-2*) and Table S2 (*ago4-3*). For the rest of RNA-seq analyses, after evaluating differential expression using EDGER, genes were selected with an absolute log₂FC greater than 1.5 and a false discovery rate (FDR) smaller than 1e⁻⁴. Heat maps were generated using the HEAT-MAP.2 package in R; logarithms of counts per million (CPM) were standardized across genes (rows), and thus converted to standard deviations (SDs) from the mean (z-score). The standardized values were also used to cluster genes by the similarity of their profiles over samples. To find genes for which induction or repression by salt is stronger in a mutant than in the wild type, we used a 'the differential response to NaCl' score ('diff'), which subtracts the effect of salt in the wild type from the effect of salt in the mutant, as follows: diff = log₂('FC *ago4* NaCl versus *ago4* MS') – log₂('FC Col-0 NaCl versus Col-0 MS').

To select the most affected genes in the *ago4-2* and *ago4-3* mutants, diff was standardized across all genes for each mutant, and genes for which diff is 3.0 or more SD above the mean were considered hyperinduced (upregulated), and those for which diff is 3.0 or more SD below the mean were considered hyperrepressed (downregulated). Diff values for the selected genes are reported in Tables S3–S6. The selected genes are also shown in Figure S12(b–e).

Whole-genome bisulfite sequencing (WGBS)

DNA from the lines and conditions described for the RNA-seq, plus *nrpe1*, was isolated using the DNeasy Plant mini kit (Qiagen, <https://www.qiagen.com>) following the manufacturer's protocol, with minor changes to handle low-input samples. DNA quality was assessed by 0.8% agarose gel electrophoresis as a single band above 20 Kb. Portions of DNA (100 ng) were used to generate sequencing libraries using the Methyl-seq Pico Library Prep kit (Zymo, <https://www.zymoresearch.com>) following the manufacturer's instructions. Non-directional DNA libraries were single barcoded and sequenced with its biological duplicate in two lanes of the HiSeq X-Ten platform (Illumina) with a 2 × 150 paired-end (PE) configuration. Sequencing was performed by the HudsonAlpha Institute for Biotechnology (<https://hudsonalpha.org>). The WGBS libraries for the *nrpe1* mutant were sequenced in a NovaSeq S4 flow-cell at the Advanced Genomics Core of the University of Michigan with a 2 × 150 PE configuration.

WGBS analysis

Following sequencing, all libraries contained between 40 and 82 million high-quality reads. Reads were adapter-trimmed using

TRIM GALORE (Chen *et al.*, 2014), and subsequently mapped using BIS-MARK (Krueger and Andrews, 2011) with the BOWTIE2 PE alignment option. Genome coverage higher than 20× was obtained with a bisulfite conversion higher than 99.1%, assessed by analyzing cytosine methylation in the plastid genome. Analysis of DNA methylation and differentially methylated regions (DMRs) calling were done using the methyl-Kit R package (Akalin *et al.*, 2012). DMRs were defined as a 10% statistically significant (FDR = 0.01) methylation difference between samples using 100-bp sliding windows (50 bp step size). Regions with at least 10 reads were considered for the downstream analysis. Overlapping and cross-analysis of DMRs and genomic features, and the RNA-seq and WGBS, respectively, were performed using BEDTOOLS. Genomic features for overlapping analyses were taken from the TAIR database (<https://www.arabidopsis.org>) and are based on gene type, including protein-coding genes, pseudogenes, transposable element genes, transposon fragments, non-coding RNAs, small nucleolar RNAs, microRNA, ribosomal RNAs, etc.

All box plots and heat maps were generated using R. The TAIR 10 version of the genome was used as a reference for mapping and as a reference for the genomic models used in the comparisons performed in this work.

ACKNOWLEDGEMENTS

This work was partially supported by a grant from Programa de Apoyo a Proyectos de Investigación e Innovación Tecnológica de la Universidad Nacional Autónoma de México (PAPIIT-UNAM) (IN211816). We are grateful to Andrzej Wierzbicki for his support during the development of this work and for his critical reading of the manuscript and comments. We also thank Caspar Chater, Tzvetanka D. Dinkova and M. Hafiz Rothi for their critical reading of the manuscript and for valuable comments, and P. Vera, Y. Qi, M.J. Axtel, J.K. Zhu and B. Meyers for the generous gift of some of the seeds used in this work, as indicated in the text. We also thank the Unidad Universitaria de Secuenciación Masiva y Bioinformática, Unidad de Síntesis y Secuenciación de DNA, to the Laboratorio Nacional de Microscopía Avanzada, R. Grande, V. Jiménez-Jacinto, K. Estrada-Guerra, C.L. Ibarra-Sánchez, C.A. González-Chávez, R.M. Solórzano and M.B. Pérez-Morales for their technical support. We are also thankful to A. Cruz for the preliminary phenotypical analysis in Arabidopsis roots. VMP and CM-M received PhD and MSc fellowships, respectively, from Consejo Nacional de Ciencia y Tecnología (CONACyT)-México, and ORB was the recipient of a predoctoral fellowship from Instituto de Biotecnología. VMP is a doctoral student from Programa de Doctorado en Ciencias Biomédicas, Universidad Nacional Autónoma de México and has received a CONACyT fellowship (239759).

AUTHOR CONTRIBUTIONS

VMP and AAC conceived the idea and designed the research. VMP, AAC and JLR interpreted the data and wrote the article. VMP performed germination and immunodetection experiments with the help of ORB. AGA performed the root-length experiments. VMP, AG and AAC analyzed the RNA-seq data. CM-M performed the fluorescence imaging, with the assistance of VMP. VMP performed, analyzed and interpreted the WGBS data with the assistance of AAC. All authors reviewed the article and approved the final version for publication.

CONFLICT OF INTEREST

The authors declare that they have no competing financial interests.

DATA AVAILABILITY STATEMENT

The RNA-seq data generated in this work can be freely accessed through the Gene Expression Omnibus (GEO, <https://www.ncbi.nlm.nih.gov/geo/>) project GSE112051. The WGBS data can be found in project GSE156093. The RIP-seq data set (Bohmdorfer *et al.*, 2016) used in this work to analyze the Pol V transcribed region proximity can be accessed in GEO project GSE70290.

SUPPORTING INFORMATION

Additional Supporting Information may be found in the online version of this article.

Figure S1. Germination of the Arabidopsis lines displayed in Figure 1, under optimal conditions.

Figure S2. Germination of additional AGO4 null mutant lines on different genetic backgrounds.

Figure S3. Western blot immunodetection of AGO4 protein in the different Arabidopsis lines used in this study.

Figure S4. Dose-dependency effect of salt treatments on the RdDM core protein mutants during germination.

Figure S5. Effect of AGO4 mutants on root growth.

Figure S6. Comparison of transcript accumulation among the AGO4/6/9 clade.

Figure S7. AGO4 intracellular localization in germinating seeds.

Figure S8. AGO4 localization in the root apical region.

Figure S9. Genome-wide DNA methylation analyses comparing RdDM mutants with the wild type (Col-0).

Figure S10. Locus-specific DNA methylation differences in RdDM mutants.

Figure S11. Identification of RdDM direct targets in *ago4-3*.

Figure S12. RNA-seq transcriptome analysis of *ago4-2* and *ago4-3* mutants in response to salinity.

Table S1. List of DMR numbers identified for AGO4 and NRPE1 mutants.

Table S2. List of candidate genes directly modulated by RdDM in *ago4-3*.

Table S3. List of specific *ago4-3* salt upregulated genes.

Table S4. List of specific *ago4-3* salt downregulated genes.

Table S5. List of specific *ago4-2* salt upregulated genes.

Table S6. List of specific *ago4-2* salt downregulated genes.

REFERENCES

- Agorio, A. and Vera, P. (2007) ARGONAUTE4 is required for resistance to *Pseudomonas syringae* in Arabidopsis. *Plant Cell*, **19**, 3778–3790.
- Akalin, A., Kormaksson, M., Li, S., Garrett-Bakelman, F.E., Figueroa, M.E., Melnick, A. and Mason, C.E. (2012) methylKit: a comprehensive R package for the analysis of genome-wide DNA methylation profiles. *Genome Biol.* **13**, R87.
- Au, P.C.K., Dennis, E.S. and Wang, M.B. (2017) Analysis of Argonaute 4-associated long non-coding RNA in Arabidopsis thaliana sheds novel insights into gene regulation through RNA-directed DNA methylation. *Genes*, **8**, 198.

- Becerra, C., Jahrmann, T., Puigdomènech, P. and Vicient, C.M. (2004) Ankyrin repeat-containing proteins in Arabidopsis: characterization of a novel and abundant group of genes coding ankyrin-transmembrane proteins. *Gene*, **340**(1), 111–121.
- Binder, B.M., Walker, J.M., Gagne, J.M., Emborg, T.J., Hemmann, G., Bleecker, A.B. and Vierstra, R.D. (2007) The Arabidopsis EIN3 binding F-Box proteins EBF1 and EBF2 have distinct but overlapping roles in ethylene signaling. *Plant Cell*, **19**, 509–523.
- Blevins, T., Podicheti, R., Mishra, V., Marasco, M., Wang, J., Rusch, D., Tang, H. and Pikaard, C.S. (2015) Identification of Pol IV and RDR2-dependent precursors of 24 nt siRNAs guiding de novo DNA methylation in Arabidopsis. *eLife*, **4**, e09591.
- Bohmdorfer, G., Sethuraman, S., Rowley, M.J., Krzysztos, M., Rothi, M.H., Bouzit, L. and Wierzbicki, A.T. (2016) Long non-coding RNA produced by RNA polymerase V determines boundaries of heterochromatin. *eLife*, **5**, e19092.
- Borges, F., Parent, J.-S., van Ex, F., Wolff, P., Martinez, G., Köhler, C. and Martienssen, R.A. (2018) Transposon-derived small RNAs triggered by miR845 mediate genome dosage response in Arabidopsis. *Nat. Genet.* **50**, 186–192.
- Brousseau, C., El Oirdi, M., Adurogbanga, A., Ma, X. and Moffett, P. (2016) Antiviral defense involves AGO4 in an arabidopsis-potyvirus interaction. *Mol. Plant Microbe Interact.* **29**, 878–888.
- Chan, Z., Wang, Y., Cao, M., Gong, Y., Mu, Z., Wang, H., Hu, Y., Deng, X., He, X.J. and Zhu, J.K. (2016) RDM4 modulates cold stress resistance in Arabidopsis partially through the CBF-mediated pathway. *New Phytol.* **209**, 1527–1539.
- Chen, C., Khaleel, S.S., Huang, H. and Wu, C.H. (2014) Software for pre-processing Illumina next-generation sequencing short read sequences. *Source Code Biol. Med.* **9**, 8.
- Cheng, Y., Zhou, Y., Yang, Y. *et al.* (2012) Structural and functional analysis of VQ motif-containing proteins in Arabidopsis as interacting proteins of WRKY transcription factors. *Plant Physiol.* **159**(2), 810–825.
- Chinnusamy, V. and Zhu, J.K. (2009) Epigenetic regulation of stress responses in plants. *Curr. Opin. Plant Biol.* **12**, 133–139.
- Chow, H.T., Chakraborty, T. and Mosher, R.A. (2020) RNA-directed DNA Methylation and sexual reproduction: expanding beyond the seed. *Curr. Opin. Plant Biol.* **54**, 11–17.
- Corbineau, F., Xia, Q., Bailly, C. and El-Maarouf-Bouteau, H. (2014) Ethylene, a key factor in the regulation of seed dormancy. *Front. Plant Sci.* **5**, 539.
- Corem, S., Doron-Faigenboim, A., Jouffroy, O., Maumus, F., Arazi, T. and Bouche, N. (2018) Redistribution of CHH methylation and small interfering RNAs across the genome of tomato ddm1 mutants. *Plant Cell*, **30**, 1628–1644.
- Cubas, P., Vincent, C. and Coen, E. (1999) An epigenetic mutation responsible for natural variation in floral symmetry. *Nature*, **401**, 157–161.
- Cutler, S.R., Rodriguez, P.L., Finkelstein, R.R. and Abrams, S.R. (2010) Abscisic acid: emergence of a core signaling network. *Annu. Rev. Plant Biol.* **61**, 651–679.
- Downen, R.H., Pelizzola, M., Schmitz, R.J., Lister, R., Downen, J.M., Nery, J.R., Dixon, J.E. and Ecker, J.R. (2012) Widespread dynamic DNA methylation in response to biotic stress. *Proc. Natl Acad. Sci. USA*, **109**, E2183–2191.
- Duan, C.G., Zhang, H., Tang, K. *et al.* (2015) Specific but interdependent functions for Arabidopsis AGO4 and AGO6 in RNA-directed DNA methylation. *EMBO J.* **34**, 581–592.
- Eun, C., Lorkovic, Z.J., Naumann, U., Long, Q., Havecker, E.R., Simon, S.A., Meyers, B.C., Matzke, A.J. and Matzke, M. (2011) AGO6 functions in RNA-mediated transcriptional gene silencing in shoot and root meristems in Arabidopsis thaliana. *PLoS One*, **6**, e25730.
- Faus, I., Ninoles, R., Kesari, V., Llabata, P., Tam, E., Nebauer, S.G., Santiago, J., Hauser, M.T. and Gadea, J. (2018) Arabidopsis ILTHYIA protein is necessary for proper chloroplast biogenesis and root development independent of eIF2 α phosphorylation. *J. Plant Physiol.* **224–225**, 173–182.
- Gallego-Bartolome, J., Liu, W., Kuo, P.H., Feng, S., Ghoshal, B., Gardiner, J., Zhao, J.M., Park, S.Y., Chory, J. and Jacobsen, S.E. (2019) Co-targeting RNA polymerases IV and V promotes efficient de novo DNA methylation in Arabidopsis. *Cell*, **176**(5), 1068–1082.e19.
- Gao, Y.Q., Chen, J.G., Chen, Z.R., An, D., Lv, Q.Y., Han, M.L., Wang, Y.L., Salt, D.E. and Chao, D.Y. (2017) A new vesicle trafficking regulator CTL1 plays a crucial role in ion homeostasis. *PLoS Biol.* **15**(12), e2002978.
- Gissot, L., Polge, C., Jossier, M., Girin, T., Bouly, J.P., Kreis, M. and Thomas, M. (2006) AKINbetagamma contributes to SnRK1 heterotrimeric complexes and interacts with two proteins implicated in plant pathogen resistance through its KIS/GBD sequence. *Plant Physiol.* **142**(3), 931–944.
- Gohlke, J., Scholz, C.J., Kneitz, S., Weber, D., Fuchs, J., Hedrich, R. and Deeken, R. (2013) DNA methylation mediated control of gene expression is critical for development of crown gall tumors. *PLoS Genet.* **9**, e1003267.
- Gouil, Q. and Baulcombe, D.C. (2016) DNA methylation signatures of the plant chromomethyltransferases. *PLoS Genet.* **12**, e1006526.
- Grover, J.W., Kendall, T., Baten, A., Burgess, D., Freeling, M., King, G.J. and Mosher, R.A. (2018) Maternal components of RNA-directed DNA methylation are required for seed development in Brassica rapa. *Plant J.* **94**, 575–582.
- Haag, J.R. and Pikaard, C.S. (2011) Multisubunit RNA polymerases IV and V: purveyors of non-coding RNA for plant gene silencing. *Nat. Rev. Mol. Cell Biol.* **12**, 483–492.
- Hamera, S., Song, X., Su, L., Chen, X. and Fang, R. (2012) Cucumber mosaic virus suppressor 2b binds to AGO4-related small RNAs and impairs AGO4 activities. *Plant J.* **69**, 104–115.
- Han, S.K. and Wagner, D. (2014) Role of chromatin in water stress responses in plants. *J. Exp. Bot.* **65**, 2785–2799.
- Havecker, E.R., Wallbridge, L.M., Hardcastle, T.J., Bush, M.S., Kelly, K.A., Dunn, R.M., Schwach, F., Doonan, J.H. and Baulcombe, D.C. (2010) The Arabidopsis RNA-directed DNA methylation argonauts functionally diverge based on their expression and interaction with target loci. *Plant Cell*, **22**, 321–334.
- Henderson, I.R., Zhang, X., Lu, C., Johnson, L., Meyers, B.C., Green, P.J. and Jacobsen, S.E. (2006) Dissecting Arabidopsis thaliana DICER function in small RNA processing, gene silencing and DNA methylation patterning. *Nat. Genet.* **38**, 721–725.
- Hollick, J.B. (2010) Paramutation and development. *Annu. Rev. Cell Dev. Biol.* **26**, 557–579.
- Ito, H., Gaubert, H., Bucher, E., Mirouze, M., Vaillant, I. and Paszkowski, J. (2011) An siRNA pathway prevents transgenerational retrotransposition in plants subjected to stress. *Nature*, **472**, 115–119.
- Iwasaki, M., Hyvärinen, L., Piskurewicz, U. and Lopez-Molina, L. (2019) Non-canonical RNA-directed DNA methylation participates in maternal and environmental control of seed dormancy. *eLife*, **8**, e37434.
- Jacobs, J. and Roe, J.L. (2005) SKS6, a multicopper oxidase-like gene, participates in cotyledon vascular patterning during Arabidopsis thaliana development. *Planta*, **222**, 652–666.
- Jing, Y. and Lin, R. (2015) The VQ motif-containing protein family of plant-specific transcriptional regulators. *Plant Physiol.* **169**(1), 371–378.
- Kawakatsu, T., Nery, J.R., Castanon, R. and Ecker, J.R. (2017) Dynamic DNA methylation reconfiguration during seed development and germination. *Genome Biol.* **18**, 171.
- Kawakatsu, T., Stuart, T., Valdes, M. *et al.* (2016) Unique cell-type-specific patterns of DNA methylation in the root meristem. *Nat. Plants*, **2**, 16058.
- Kinoshita, T. and Seki, M. (2014) Epigenetic memory for stress response and adaptation in plants. *Plant Cell Physiol.* **55**, 1859–1863.
- Kirkbride, R.C., Lu, J., Zhang, C., Mosher, R.A., Baulcombe, D.C. and Chen, Z.J. (2019) Maternal small RNAs mediate spatial-temporal regulation of gene expression, imprinting, and seed development in Arabidopsis. *Proc. Natl Acad. Sci. USA*, **116**, 2761–2766.
- Köhler, C. and Lafon-Placette, C. (2015) Evolution and function of epigenetic processes in the endosperm. *Front. Plant Sci.* **6**, 130.
- Kradolfer, D., Wolff, P., Jiang, H., Siretskiy, A. and Kohler, C. (2013) An imprinted gene underlies postzygotic reproductive isolation in Arabidopsis thaliana. *Dev. Cell*, **26**, 525–535.
- Krueger, F. and Andrews, S.R. (2011) Bismark: a flexible aligner and methylation caller for Bisulfite-Seq applications. *Bioinformatics*, **27**, 1571–1572.
- Kurihara, Y., Matsui, A., Kawashima, M. *et al.* (2008) Identification of the candidate genes regulated by RNA-directed DNA methylation in Arabidopsis. *Biochem. Biophys. Res. Commun.* **376**, 553–557.
- Law, J.A. and Jacobsen, S.E. (2010) Establishing, maintaining and modifying DNA methylation patterns in plants and animals. *Nat. Rev. Genet.* **11**, 204–220.
- Le, T.N., Schumann, U., Smith, N.A. *et al.* (2014) DNA demethylases target promoter transposable elements to positively regulate stress responsive genes in Arabidopsis. *Genome Biol.* **15**, 458.
- Lee, M.H., Jeon, H.S., Kim, H.G. and Park, O.K. (2017) An Arabidopsis NAC transcription factor NAC4 promotes pathogen-induced cell death under negative regulation by microRNA164. *New Phytol.* **214**, 343–360.

- Leubner-Metzger, G., Petruzzelli, L., Waldvogel, R., Vogeli-Lange, R. and Meins, F. Jr (1998) Ethylene-responsive element binding protein (EREBP) expression and the transcriptional regulation of class I beta-1,3-glucanase during tobacco seed germination. *Plant Mol. Biol.* **38**, 785–795.
- Li, H., Handsaker, B., Wysoker, A., Fennell, T., Ruan, J., Homer, N., Marth, G., Abecasis, G., Durbin, R.; 1000 Genome Project Data Processing Subgroup. (2009) The Sequence Alignment/Map format and SAMtools. *Bioinformatics*, **25**, 2078–2079.
- Li, X., Chen, T., Li, Y., Wang, Z., Cao, H., Chen, F., Li, Y., Soppe, W.J.J., Li, W. and Liu, Y. (2019) ETR1/RDO3 regulates seed dormancy by relieving the inhibitory effect of the ERF12-TPL complex on DELAY OF GERMINATION1 expression. *Plant Cell*, **31**, 832–847.
- Lin, Y., Yang, L., Paul, M., Zu, Y. and Tang, Z. (2013) Ethylene promotes germination of Arabidopsis seed under salinity by decreasing reactive oxygen species: evidence for the involvement of nitric oxide simulated by sodium nitroprusside. *Plant Physiol. Biochem.* **73**, 211–218.
- Liu, X., Zhang, H., Zhao, Y., Feng, Z., Li, Q., Yang, H.Q., Luan, S., Li, J. and He, Z.H. (2013) Auxin controls seed dormancy through stimulation of abscisic acid signaling by inducing ARF-mediated ABI3 activation in Arabidopsis. *Proc. Natl Acad. Sci. USA*, **110**, 15485–15490.
- Lopez, A., Ramirez, V., Garcia-Andrade, J., Flors, V. and Vera, P. (2011) The RNA silencing enzyme RNA polymerase v is required for plant immunity. *PLoS Genet.* **7**, e1002434.
- Lowry, O.H., Rosebrough, N.J., Farr, A.L. and Randall, R.J. (1951) Protein measurement with the Folin phenol reagent. *J. Biol. Chem.* **193**, 265–275.
- Mahfouz, M.M. (2010) RNA-directed DNA methylation: mechanisms and functions. *Plant Signal. Behav.* **5**, 806–816.
- Manning, K., Tor, M., Poole, M., Hong, Y., Thompson, A.J., King, G.J., Giovannoni, J.J. and Seymour, G.B. (2006) A naturally occurring epigenetic mutation in a gene encoding an SBP-box transcription factor inhibits tomato fruit ripening. *Nat. Genet.* **38**, 948–952.
- Martinez, G., Wolff, P., Wang, Z., Moreno-Romero, J., Santos-Gonzalez, J., Conze, L.L., Defraia, C., Slotkin, R.K. and Kohler, C. (2018) Paternal easiRNAs regulate parental genome dosage in Arabidopsis. *Nat. Genet.* **50**, 193–198.
- Matsunaga, W., Kobayashi, A., Kato, A. and Ito, H. (2012) The effects of heat induction and the siRNA biogenesis pathway on the transgenerational transposition of ONSEN, a copia-like retrotransposon in Arabidopsis thaliana. *Plant Cell Physiol.* **53**, 824–833.
- Matzke, M.A., Kanno, T. and Matzke, A.J. (2015) RNA-directed DNA methylation: the evolution of a complex epigenetic pathway in flowering plants. *Annu. Rev. Plant Biol.* **66**, 243–267.
- Matzke, M.A. and Mosher, R.A. (2014) RNA-directed DNA methylation: an epigenetic pathway of increasing complexity. *Nat. Rev. Genet.* **15**, 394–408.
- Maurer-Stroh, S., Dickens, N.J., Hughes-Davies, L., Kouzarides, T., Eisenhaber, F. and Ponting, C.P. (2003) The Tudor domain 'Royal Family': Tudor, plant Aget, Chromo, PWWP and MBT domains. *Trends Biochem. Sci.* **28**(2), 69–74.
- McCue, A.D., Panda, K., Nuthikattu, S., Choudury, S.G., Thomas, E.N. and Slotkin, R.K. (2015) ARGONAUTE 6 bridges transposable element mRNA-derived siRNAs to the establishment of DNA methylation. *EMBO J.* **34**, 20–35.
- Melnyk, C.W., Molnar, A. and Baulcombe, D.C. (2011) Intercellular and systemic movement of RNA silencing signals. *EMBO J.* **30**, 3553–3563.
- Merchante, C., Alonso, J.M. and Stepanova, A.N. (2013) Ethylene signaling: simple ligand, complex regulation. *Curr. Opin. Plant Biol.* **16**, 554–560.
- Molinier, J., Ries, G., Zipfel, C. and Hohn, B. (2006) Transgeneration memory of stress in plants. *Nature*, **442**, 1046–1049.
- Myline, J.S., Wang, C.K., van der Weerden, N.L. and Craik, D.J. (2010) Cycloptides are a component of the innate defense of Oldenlandia affinis. *Biopolymers*, **94**, 635–646.
- Nakashima, K., Ito, Y. and Yamaguchi-Shinozaki, K. (2009) Transcriptional regulatory networks in response to abiotic stresses in Arabidopsis and grasses. *Plant Physiol.* **149**, 88–95.
- Nee, G., Kramer, K., Nakabayashi, K., Yuan, B., Xiang, Y., Miatton, E., Finke-meier, I. and Soppe, W.J.J. (2017) DELAY OF GERMINATION1 requires PP2C phosphatases of the ABA signalling pathway to control seed dormancy. *Nat. Commun.* **8**, 72.
- Nishimura, N., Tsuchiya, W., Moresco, J.J. et al. (2018) Control of seed dormancy and germination by DOG1-AHG1 PP2C phosphatase complex via binding to heme. *Nat. Commun.* **9**, 2132.
- Nishimura, N., Yoshida, T., Kitahata, N., Asami, T., Shinozaki, K. and Hirayama, T. (2007) ABA-hypersensitive Germination1 encodes a protein phosphatase 2C, an essential component of abscisic acid signaling in Arabidopsis seed. *Plant J.* **50**, 935–949.
- Olmedo-Monfil, V., Duran-Figueroa, N., Arteaga-Vazquez, M., Demesa-Arevalo, E., Autran, D., Grimanelli, D., Slotkin, R.K., Martienssen, R.A. and Vielle-Calzada, J.P. (2010) Control of female gamete formation by a small RNA pathway in Arabidopsis. *Nature*, **464**, 628–632.
- Olvera-Carrillo, Y., Campos, F., Reyes, J.L., Garcarrubio, A. and Covarrubias, A.A. (2010) Functional analysis of the group 4 late embryogenesis abundant proteins reveals their relevance in the adaptive response during water deficit in Arabidopsis. *Plant Physiol.* **154**, 373–390.
- Pecinka, A. and Mittelsten Scheid, O. (2012) Stress-induced chromatin changes: a critical view on their heritability. *Plant Cell Physiol.* **53**, 801–808.
- Pirrello, J., Jaimes-Miranda, F., Sanchez-Ballesta, M.T., Tournier, B., Khalil-Ahmad, Q., Regad, F., Latche, A., Pech, J.C. and Bouzayen, M. (2006) SLERF2, a tomato ethylene response factor involved in ethylene response and seed germination. *Plant Cell Physiol.* **47**, 1195–1205.
- Pontier, D., Yahubyan, G., Vega, D., Bulski, A., Saez-Vasquez, J., Hakimi, M.A., Lerbs-Mache, S., Colot, V. and Lagrange, T. (2005) Reinforcement of silencing at transposons and highly repeated sequences requires the concerted action of two distinct RNA polymerases IV in Arabidopsis. *Genes Dev.* **19**, 2030–2040.
- Popova, O.V., Dinh, H.Q., Aufsatz, W. and Jonak, C. (2013) The RdDM pathway is required for basal heat tolerance in Arabidopsis. *Mol. Plant*, **6**, 396–410.
- Robinson, M.D. and Smyth, G.K. (2008) Small-sample estimation of negative binomial dispersion, with applications to SAGE data. *Biostatistics*, **9**, 321–332.
- Sarkies, P. and Miska, E.A. (2014) Small RNAs break out: the molecular cell biology of mobile small RNAs. *Nat. Rev. Mol. Cell Biol.* **15**, 525–535.
- Schoft, V.K., Chumak, N., Mosiolek, M., Slusarz, L., Komnenovic, V., Brownfield, L., Twell, D., Kakutani, T. and Tamaru, H. (2009) Induction of RNA-directed DNA methylation upon decondensation of constitutive heterochromatin. *EMBO Rep.* **10**, 1015–1021.
- Secco, D., Wang, C., Shou, H., Schultz, M.D., Chiarenza, S., Nussaume, L., Ecker, J.R., Whelan, J. and Lister, R. (2015) Stress induced gene expression drives transient DNA methylation changes at adjacent repetitive elements. *eLife*, **4**, e09343.
- Skirycz, A. and Inze, D. (2010) More from less: plant growth under limited water. *Curr. Opin. Biotechnol.* **21**, 197–203.
- Soppe, W.J., Jacobsen, S.E., Alonso-Blanco, C., Jackson, J.P., Kakutani, T., Koornneef, M. and Peeters, A.J. (2000) The late flowering phenotype of fwa mutants is caused by gain-of-function epigenetic alleles of a homeodomain gene. *Mol. Cell*, **6**, 791–802.
- Sun, L., Zhang, P., Wang, R., Wan, J., Ju, Q., Rothstein, S.J. and Xu, J. (2019) The SNAC-A transcription factor ANAC032 reprograms metabolism in Arabidopsis. *Plant Cell Physiol.* **60**, 999–1010.
- Thomas, C.L., Bayer, E.M., Ritzenthaler, C., Fernandez-Calvino, L. and Maule, A.J. (2008) Specific targeting of a plasmodesmal protein affecting cell-to-cell communication. *PLoS Biol.* **6**, e7.
- Tricker, P.J., Gibbings, J.G., Rodriguez Lopez, C.M., Hadley, P. and Wilkinson, M.J. (2012) Low relative humidity triggers RNA-directed de novo DNA methylation and suppression of genes controlling stomatal development. *J. Exp. Bot.* **63**, 3799–3813.
- Vidal, E.A., Alvarez, J.M. and Gutierrez, R.A. (2014) Nitrate regulation of AFB3 and NAC4 gene expression in Arabidopsis roots depends on NRT1.1 nitrate transport function. *Plant Signal. Behav.* **9**, e28501.
- Vidal, E.A., Moyano, T.C., Riveras, E., Contreras-López, O. and Gutiérrez, R.A. (2013) Systems approaches map regulatory networks downstream of the auxin receptor AFB3 in the nitrate response of Arabidopsis thaliana roots. *Proc. Natl. Acad. Sci. USA* **110**(31), 12840–12845.
- Wang, F. and Axtell, M.J. (2017) AGO4 is specifically required for heterochromatic siRNA accumulation at Pol V-dependent loci in Arabidopsis thaliana. *Plant J.* **90**, 37–47.
- Wang, G. and Köhler, C. (2017) Epigenetic processes in flowering plant reproduction. *J. Exp. Bot.* **68**, 797–807.
- Wang, Y., Liu, C., Li, K. et al. (2007) Arabidopsis EIN2 modulates stress response through abscisic acid response pathway. *Plant Mol. Biol.* **64**, 633–644.

- Wang, Z., Butel, N., Santos-Gonzalez, J., Borges, F., Yi, J., Martienssen, R.A., Martinez, G. and Kohler, C. (2020) Polymerase IV plays a crucial role in pollen development in *capsella*. *Plant Cell*, **32**, 950–966.
- Wei, L., Gu, L., Song, X. *et al.* (2014) Dicer-like 3 produces transposable element-associated 24-nt siRNAs that control agricultural traits in rice. *Proc. Natl Acad. Sci. USA*, **111**, 3877–3882.
- Wierzbicki, A.T., Cocklin, R., Mayampurath, A., Lister, R., Rowley, M.J., Gregory, B.D., Ecker, J.R., Tang, H. and Pikaard, C.S. (2012) Spatial and functional relationships among Pol V-associated loci, Pol IV-dependent siRNAs, and cytosine methylation in the *Arabidopsis* epigenome. *Genes Dev.* **26**, 1825–1836.
- Wierzbicki, A.T., Ream, T.S., Haag, J.R. and Pikaard, C.S. (2009) RNA polymerase V transcription guides ARGONAUTE4 to chromatin. *Nat. Genet.* **41**, 630–634.
- Winter, V. and Hauser, M.T. (2006) Exploring the ESCRTing machinery in eukaryotes. *Trends Plant Sci.* **11**(3), 115–123.
- Wu, L., Zhou, H., Zhang, Q., Zhang, J., Ni, F., Liu, C. and Qi, Y. (2010) DNA methylation mediated by a microRNA pathway. *Mol. Cell*, **38**, 465–475.
- Yaari, R., Katz, A., Domb, K., Harris, K.D., Zemach, A. and Ohad, N. (2019) RdDM-independent de novo and heterochromatin DNA methylation by plant CMT and DNMT3 orthologs. *Nat. Commun.* **10**, 1613.
- Yamaguchi-Shinozaki, K. and Shinozaki, K. (2006) Transcriptional regulatory networks in cellular responses and tolerance to dehydration and cold stresses. *Annu. Rev. Plant Biol.* **57**, 781–803.
- Yang, L.P., Fang, Y.Y., An, C.P., Dong, L., Zhang, Z.H., Chen, H., Xie, Q. and Guo, H.S. (2013) C2-mediated decrease in DNA methylation, accumulation of siRNAs, and increase in expression for genes involved in defense pathways in plants infected with beet severe curly top virus. *Plant J.* **73**, 910–917.
- Ye, R., Wang, W., Iki, T., Liu, C., Wu, Y., Ishikawa, M., Zhou, X. and Qi, Y. (2012) Cytoplasmic assembly and selective nuclear import of *Arabidopsis* Argonaute4/siRNA complexes. *Mol. Cell*, **46**, 859–870.
- Zhai, J., Bischof, S., Wang, H. *et al.* (2015) A one precursor one siRNA model for Pol IV-dependent siRNA biogenesis. *Cell*, **163**, 445–455.
- Zhang, H. and Zhu, J.K. (2012) Seeing the forest for the trees: a wide perspective on RNA-directed DNA methylation. *Genes Dev.* **26**, 1769–1773.
- Zheng, Q., Rowley, M.J., Bohmdorfer, G., Sandhu, D., Gregory, B.D. and Wierzbicki, A.T. (2013) RNA polymerase V targets transcriptional silencing components to promoters of protein-coding genes. *Plant J.* **73**, 179–189.
- Zhu, J.K. (2002) Salt and drought stress signal transduction in plants. *Annu. Rev. Plant Biol.* **53**, 247–273.
- Zilberman, D., Cao, X. and Jacobsen, S.E. (2003) ARGONAUTE4 control of locus-specific siRNA accumulation and DNA and histone methylation. *Science*, **299**, 716–719.